Detecting Symmetry and Symmetric Constellations of Features

Gareth Loy[*] and Jan-Olof Eklundh

Computational Vision & Active Perception Laboratory,
Royal Institute of Technology (KTH), Sweden
{gareth, joe}@nada.kth.se

Abstract. A novel and efficient method is presented for grouping feature points on the basis of their underlying symmetry and characterising the symmetries present in an image. We show how symmetric pairs of features can be efficiently detected, how the symmetry bonding each pair is extracted and evaluated, and how these can be grouped into symmetric constellations that specify the dominant symmetries present in the image. Symmetries over all orientations and radii are considered simultaneously, and the method is able to detect local or global symmetries, locate symmetric figures in complex backgrounds, detect bilateral or rotational symmetry, and detect multiple incidences of symmetry.

1 Introduction

Symmetry is an intrinsic phenomenon in the world around us, occurring both naturally and in artefacts and architecture. Symmetry is attractive, both aesthetically and as a cue directing visual attention [2, 8, 15, 27]. Not only does it give balance and form to appearance, but it ties together features that can otherwise seem diffuse. With the recent success of feature point methods in computer vision [9, 16, 21, 22] it is useful to establish mechanisms for grouping the features generated, and symmetry provides a natural means of doing so.

The contribution of this paper is a simple and effective method for grouping symmetric constellations of features and detecting symmetry in the image plane. Modern feature-based methods (such as [9, 16]) are used to establish pairs of symmetric point matches from which either bilateral symmetry axes or centres of rotational symmetry can be analytically determined. These pairs are grouped into symmetric constellations of features about common symmetry foci, identifying both the dominant symmetries present and a set features associated with each foci. The method is independent of the feature detector and descriptor used, requiring only robust, rotation-invariant matching and an orientation measure for each feature. Symmetries over all orientations and radii are considered simultaneously, and the method can also detect multiple axes of symmetry, rotational symmetry and symmetric figures in complex backgrounds.

The remainder of this paper is organised as follows, Section 2 reviews previous work, Section 3 describes the method, Section 4 presents experimental results and discusses the performance of the method, and Section 5 presents our conclusions.

---

2   Background

Symmetry has fascinated people since ancient times, and in the computer vision literature there is a significant body of work dealing with the detection of symmetry in images dating back to the 1970's (e.g. [3, 10, 17, 19, 20, 24, 30, 31, 35, 37]). Symmetry detection has been used for numerous applications, including facial image analysis [23], vehicle detection [12, 38], reconstruction [1, 6, 14, 34], visual attention [17, 24, 27] indexing of image databases [28], completion of occluded shapes [36], object detection [19, 37] and detecting tumours in medical imaging [18]. The problem of symmetry detection amounts to trying to find an image region of unknown size that, when flipped about an unknown axis or rotated about an unknown point, is sufficiently similar to another image region an unknown distance away. With so many unknown parameters it is not surprising that symmetry detection is a complex task.

Some researchers have taken a global approach to the problem, treating the entire image as a signal from which symmetric properties are inferred, often via frequency analysis. Marola [19] proposed a method for detecting symmetry in symmetric and "almost symmetric" images, where the axis of symmetry intersects or passes near the centroid. Keller and Shkolnisky [10] took an algebraic approach and employed Fourier analysis to detect symmetry, and Sun [31] showed that the orientation of the dominant bilateral symmetry axis could be computed from the histogram of gradient orientations. However, these global approaches have two key shortcomings: they are limited to detecting a single incidence of symmetry, and are adversely influenced by background structure.

An alternative to the global approach is to use local features such as edge features, contours or boundary points, to reduce the problem to one of grouping symmetric sets of points or lines. Scott and Longuet-Higgins [26] grouped symmetric sets of dot-patterns extracted from the wing markings of a butterfly using the eigenvectors of a proximity matrix. Masuda *et al.* [20] adopted an image similarity measure based on the directional correlation of edge features and proceeded to detect rotational and reflectional symmetry. This required an exhaustive search of all congruent transformations (consisting of translation, rotation and reflection) of an image to identify any such transformations under which parts of the image were close to invariant.

Zabrodsky *et al.* [37] proposed the *symmetry distance* as a continuous measure of the amount of symmetry present in a shape. This distance was defined as the minimum mean squared distance required to move points of the original shape to obtain a perfectly symmetrical shape, and enabled a comparison of the "amount" of symmetry present in different shapes. Given the location and orientation of a symmetry axis, this method was used in conjunction with active contours to extract symmetric regions such as faces. However, this method required the foci of symmetry to be known a priori.

Tuytelaars *et al.* [32] detected regular repetitions of planar patterns under perspective skew using a geometric framework. The approach detected all planar homologies[1] and could thus find reflections about a point, periodicities, and mirror symmetries. By considering perspective skew this method dealt with a much more general and complex problem than detection of two-dimensional symmetries within an image. Whilst this

---

[1] A plane projective transformation is a planar homology if it has a line of fixed points (called the axis), together with a fixed point (called the vertex) not on the line [5].

approach could indeed detect mirror symmetries in the image plane, it was a slow and involved means of doing so, and as posed was unable to detect rotational symmetries. This method built clusters of matching points that were evaluated for symmetry, by contrast the new method forms pairs of matching features whose symmetry can be rapidly assessed from their embedded orientation and scale information.

Lazebnik *et al.* [13] also noted that clusters of features could be matched within an image to detect symmetries. However, the use of rotationally invariant descriptors (providing no orientation information) restricted this, like [32], to a cluster-based approach.

Shen *et al.* [29] used an affine invariant representation to detect skewed symmetries in cleanly segmented contours. A set of ordered feature points is sampled around a contour and an affine invariant feature vector is constructed for each feature point. A similarity matrix is then constructed describing the similarities between the features, a threshold is applied to the matrix, and symmetries are identified as diagonal lines in the binarized similarity matrix. The method is able to detect skew symmetries and rotational symmetries, but is only suitable for pre-segmented objects and requires a strict ordering of feature points around the object contour.

Motivated by the ease with which humans and other creatures (even bees) detect symmetries, Scognamillo *et al.* [25] constructed a biologically plausible model for symmetry detection. A 2D local energy function was calculated defining a salience map of the image. The symmetry of this map was evaluated via convolution with a broad Gaussian filter oriented approximately perpendicular to the proposed axis of symmetry. Maxima were then detected in the filtered direction, and were expected to lie close to the axis of symmetry for a symmetric figure. If multiple maxima were detected the average location was used, and consequentially the method became unsuitable for detecting symmetric figures in complex backgrounds, where maxima can occur that are unrelated to the symmetric object.

Kiryati and Gofman [11] combined local and global approaches to detect the dominant reflective symmetry axis in an image. They used a symmetry measure similar to Marola [19] and applied this to assess symmetry in local circular regions parameterised by their location, size and symmetry axis orientation (x, y, s, θ). The global maximum of this measure was then determined using a probabilistic genetic algorithm which was typically able to find the global maximum of the local symmetry measure in around 1,000 iterations. As posed the method detects only a single axis of symmetry, although it is feasible to extend the genetic algorithm approach to detect multiple symmetries. However, owing to the parameterisation the method is limited to detecting circular regions of symmetry.

3   Symmetry from Feature Constellations

Our approach is based on the simple idea of matching symmetric pairs of feature points. This is achieved efficiently and robustly using modern feature point methods. The "amount" of symmetry exhibited by each pair is quantified by the relative location, orientation and scale of the features in the pair. These pair-wise symmetries are then accumulated in a Hough-style voting space to determine the dominant symmetries present in the image.

Modern feature point methods [9, 16, 21, 22] provide a proven robust means for generating dense sets of feature points and matching these between images, however, little use has been made of matching points *within* a single image. Feature point methods typically define the orientation and scale of each feature, and normalise with respect to these parameters to compute matches independent of orientation and scale. The distinctiveness of the matches obtained, together with their invariance to rotation make these methods well suited to detecting pairs of symmetric features. Rotational and translational symmetric pairs can be detected by directly matching the feature points within an image, and potential mirror symmetric matches can be obtained by constructing a set of *mirrored feature descriptors* and matching these against the original feature descriptors. Mirrored feature descriptors are defined as descriptors of mirrored copies of the local image patches associated with the original feature points (the choice of mirroring axis is arbitrary).

Matching pairs of features, mirrored or otherwise, generates a collection of matched pairs of feature points. Each feature can be represented by a point vector describing its location in x, y co-ordinates, its orientation ϕ and scale s. Symmetry can then be computed directly from these pairs of point vectors.

The remainder of this section discusses the details of this procedure for detecting bilateral and rotational symmetries.

3.1 Defining Feature Points

A set of feature points $\mathbf{p}_i$ are determined using any rotationally invariant method, such as SIFT [16], that detects distinctive points with good repeatability. Whilst a scale-invariant detection method can be used, this is not necessary. The point vector $\mathbf{p}_i = (x_i, y_i, \phi_i, s_i)$ assigned to each feature point describes its location, orientation and (optionally) scale. Scale need only be determined if a scale-invariant feature detection method is used. Orientation, however, must be determined as it is central to the evaluation of symmetry.

Next a feature descriptor $\mathbf{k}_i$ is generated for each feature point, encoding the local appearance of the feature after its orientation (and scale) have been normalised. Any feature descriptor suitable for matching can be used, see [21] for a review of leading techniques. The experiments in this paper use the SIFT descriptor [16], which gives $\mathbf{k}_i$ as a 128 element vector.

3.2 Bilateral Symmetry

A set of mirrored feature descriptors $\mathbf{m}_i$ is generated. Here $\mathbf{m}_i$ describes a mirrored version of the image patch associated with feature $\mathbf{k}_i$. The choice of mirroring axis is arbitrary owing to the orientation normalisation in the generation of the descriptor.

The mirrored feature descriptors can be generated in one of two ways. The simplest, which allows the feature detection and matching to be treated entirely as a "black box", is to flip the original image about the y (or x) axis, and compute the feature point descriptors for the mirrored image. Each mirrored feature point is then assigned to the corresponding feature point in the original image, so that $\mathbf{m}_i$ is the mirrored version of $\mathbf{k}_i$. The second, more efficient, yet slightly more involved approach requires knowledge of the configuration of the feature descriptor $\mathbf{k}_i$, and generates the mirrored feature
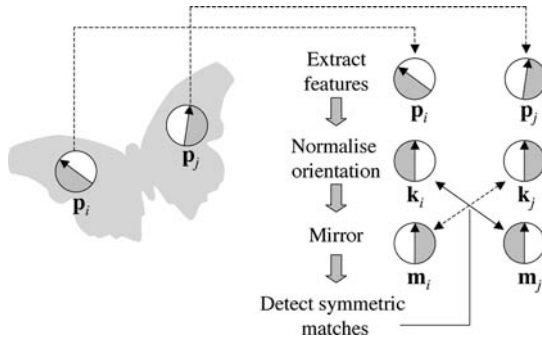
Fig. 1. Schematic illustrating the extraction and matching of a pair of symmetric features
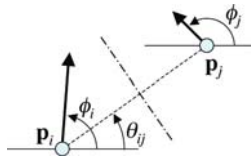

Fig. 2. A pair of point vectors $\mathbf{p}_i$ and $\mathbf{p}_j$ under scrutiny for mirror symmetry

points $\mathbf{m}_i$ by directly modifying this feature descriptor. For example, in the case of Lowe's SIFT descriptor [16] this can be achieved simply by reordering the elements of the descriptor vector so they represent the original image patch flipped about the axis aligned with the dominant orientation.

Matches are then sort between the features $\mathbf{k}_i$ and the mirrored features $\mathbf{m}_j$ to form a set of $(\mathbf{p}_i, \mathbf{p}_j)$ pairs of potentially symmetric features. Figure 1 shows a schematic of the process of extracting and matching a pair of symmetric features from an image. Each pair of symmetric features generates two matching pairs, but as these matches are equivalent only one need be recorded.

The symmetry of each pair is quantified as a function of the relative location, orientation and scale of $\mathbf{p}_i$ and $\mathbf{p}_j$. An angular symmetry weighting $\Phi_{ij} \in [-1, 1]$ (adapted from the first component of Reisfeld's [24] phase weighting function) is computed as

$$\Phi_{ij} = 1 - \cos(\phi_i + \phi_j - 2\theta_{ij}), \tag{1}$$

where the angles are defined as shown in Figure 2. A scale weighting $S_{ij} \in [0, 1]$ quantifying the relative similarity in scale of the two vectors is computed as

$$S_{ij} = \exp\left(\frac{-|s_i - s_j|}{\sigma_s(s_i + s_j)}\right)^2 \tag{2}$$

where σ_s controls the amount of scale variation accepted, $\sigma_s = 1$ was used in our experiments. Lastly an optional Gaussian distance weighting function $D_{ij} \in [0, 1]$ can be introduced to reward matching pairs that are closer to the symmetry axis. This agrees with psychophysical findings that symmetric features close to the symmetry axis contribute more to human symmetry perception than features further away [33]. However,

from a computer vision perspective introducing a distance weighting is only appropriate if a bound can be given for the diameter of symmetry to be detected, i.e., how far symmetry detection should extend perpendicular to the symmetry axis. Given such a bound σ_d the distance weighting is defined as

$$D_{ij} = \exp\left(\frac{-d^2}{2\sigma_d^2}\right) \tag{3}$$

where d is the distance separating the feature pair, otherwise $D_{ij} = 1$. Our experiments used $D_{ij} = 1$, imposing no constraint on the diameter of symmetry detected.

All these weightings are combined to form a *symmetry magnitude* for each $(\mathbf{p}_i, \mathbf{p}_j)$ pair defined by

$$M_{ij} = \begin{cases} \Phi_{ij} S_{ij} D_{ij} & \text{if } \Phi_{ij} > 0 \\ 0 & \text{otherwise} \end{cases} \tag{4}$$

The symmetry magnitude M_{ij} quantifies the "amount" of symmetry exhibited by an individual pair of point vectors. We now accumulate the symmetries exhibited by all individual pairs in a voting space to determine the dominant symmetries present in the image.

Each pair of matching points defines a potential axis of symmetry passing perpendicularly through the mid-point of the line joining $\mathbf{p}_i$ and $\mathbf{p}_j$, shown by the dash-dotted line in Figure 2. These potential symmetry axis lines can be represented using the standard $r\theta$ polar co-ordinate parameterisation with

$$r_{ij} = x_c \cos\theta_{ij} + y_c \sin\theta_{ij}$$

where (x_c, y_c) are the image centred co-ordinates of the mid-point of the line joining $\mathbf{p}_i$ and $\mathbf{p}_j$, and θ_{ij} is the angle this line subtends with the x-axis.

The linear Hough transform can then be used to find dominant symmetry axes. Each symmetric pair $(\mathbf{p}_i, \mathbf{p}_j)$ casts a vote (r_{ij}, θ_{ij}) in Hough space weighted by its symmetry magnitude M_{ij}. The resulting Hough space is blurred with a Gaussian and the maxima extracted and taken to describe the dominant symmetry axes. The points lying in the neighbourhood of these maxima in Hough space indicate the symmetric pairs that are associated with this particular axis of symmetry. The spatial extent of each symmetry axis in the image is bounded by the convex hull of the population of pairs associated with the axis.

Figure 3 shows the steps involved in computing symmetry in an example image containing a symmetric figure in a cluttered background.

This method can be adapted to detect translational symmetry by replacing the mirrored feature points with unmirrored ones and modifying the assessment of the angular symmetry weighting in Equation 1 to $\Phi_{ij} = \cos(\phi_i - \phi_j)$.

3.3   Rotational Symmetry

Unlike bilateral symmetry detection, detecting rotational symmetry does not require the manufacture of additional feature descriptors, and is detected by simply matching the features $\mathbf{k}_i$ against each other. Each match defines a pair of point vectors $(\mathbf{p}_i, \mathbf{p}_j)$. If
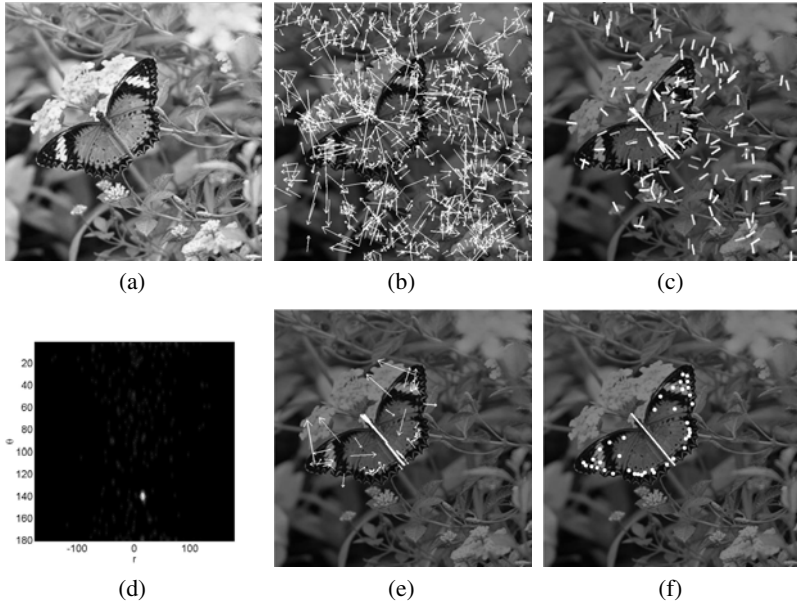
Fig. 3. Example. (a) 254×254 original image, (b) 946 feature points detected, (c) axes of symmetry associated with the 254 reflective matches obtained, intensity is proportional to symmetry magnitude M_{ij}, (d) symmetry axes in Hough space, (e) 22 symmetric features associated with the dominant symmetry axis, (f) dominant axis of symmetry and associated symmetric features.
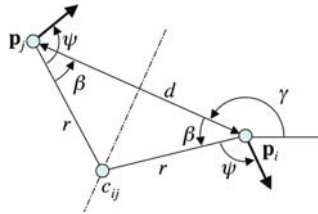

Fig. 4. Centre of rotation c_{ij} defined by point vectors $\mathbf{p}_i$ and $\mathbf{p}_j$

these vectors are parallel they do not exhibit rotational symmetry, but if they are not parallel their exists a point about which they are rotationally symmetric.

Formally, given a pair of non-parallel point vectors $\mathbf{p}_i$ and $\mathbf{p}_j$ in general position there exists a point c_{ij} a distance r from $\mathbf{p}_i$ and $\mathbf{p}_j$ about which $\mathbf{p}_i$ can be rotated to become precisely aligned and coincident with $\mathbf{p}_j$.

Figure 4 shows two such point vectors. The rotation centre c_{ij} is given by

$$c_{ij} = \begin{pmatrix} x_i \\ y_i \end{pmatrix} + \begin{pmatrix} r\cos(\beta + \gamma) \\ r\sin(\beta + \gamma) \end{pmatrix} \tag{5}$$

where x_i, y_i are the Cartesian co-ordinates of $\mathbf{p}_i$, γ is the angle the line joining $\mathbf{p}_i$ and $\mathbf{p}_j$ makes with the x-axis. By Pythagoras

$$r^2 = \left(\frac{d}{2}\right)^2 + \left(\frac{d}{2}\tan\beta\right)^2 \implies r = \frac{d\sqrt{1+\tan^2\beta}}{2},$$

where d is the distance between $\mathbf{p}_i$ and $\mathbf{p}_j$. Denoting the orientations of the point vectors $\mathbf{p}_i$ by ϕ_i, it can be seen from Figure 4 that

$$\left.\begin{array}{l} \phi_i = \gamma + \beta + \psi \\ \phi_j = \gamma + \pi - \beta + \psi \end{array}\right\} \implies \beta = \frac{\phi_i - \phi_j + \pi}{2}$$

which solves for all unknowns in Equation 5 and analytically specifies the centre of rotation of two non-parallel point vectors.

Once the centres of rotational symmetry have been determined for every matching feature pair the *rotational symmetry magnitude* R_{ij} is computed for each pair,

$$R_{ij} = S_{ij} D_{ij} \tag{6}$$

where S_{ij} is defined by Equation 2 or can be set to unity if all features have the same scale, and D_{ij} is defined by Equation 3 or is set to unity if no restriction on the size of symmetric objects to be detected is given.

Finally, the dominant centres of rotational symmetry are determined by accumulating the centres of rotation c_{ij} in a vote image the same size as the input image. Each vote is weighted by its rotational symmetry magnitude R_{ij}. The result is blurred with a Gaussian and the maxima identified as dominant centres of rotational symmetry. All centres of rotation close to a maxima are associated with that maxima.

If desired, the order of rotational symmetry can be estimated by examining the histogram of angles of rotation between matched features about each centre of rotation. Each order of rotation n defines an set of rotation angles $A = \{\frac{2\pi k}{n} : k = 1, 2, ..., n-1\}$ which should occur frequently in the angular histogram if this order of rotation is present. A simple measure of the prevalence of different rotational orders can be obtained by calculating the mean number of rotations in some vicinity q of the the angles in A and subtracting the mean number of rotations that are $\frac{2\pi(k-1)}{n}$ out of phase with these angles. This gives the order estimation function

$$O(n) = \frac{1}{n-1}\sum_{k=1}^{n-1}\sum_{-q}^{q}\left(h(\tfrac{2\pi k}{n} + q) - h(\tfrac{2\pi(k-1)}{n} + q)\right)$$

Figure 5 shows the stages towards computing rotational symmetry in an example image containing a rotationally symmetric region, (f) shows the order estimation function $O(n)$ with a clear peak at $n = 10$, and (e) shows the angular histogram with the shaded areas above and below the axis indicating the regions sampled when determining $O(n)$ for $n = 10$ (here $q = \frac{\pi}{18}$). Figure 5 (d) shows the correctly detected rotational symmetry foci of order 10, note the stray match lying off the wheel was introduced by allowing more than one match per feature, this is discussed in Section 3.4.

3.4 Matching

A similarity matrix is constructed quantifying the similarity between feature points. There are numerous ways to measure the similarity between feature vectors, for our experiments we used the Euclidean distance between the SIFT descriptors. The similarity
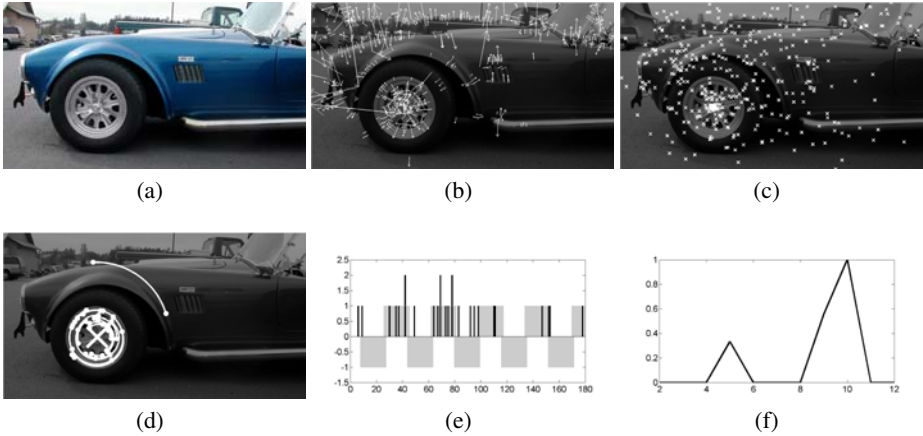
Fig. 5. Example. (a) original image, (b) feature points detected, (c) centres of rotation of matched feature pairs, (d) dominant centre of rotational symmetry and associated rotationally symmetric features, (e) histogram of angles of rotation (black) and mask applied when assessing order 10 symmetry, (f) response to detection of order of symmetry, order 10 detected.

matrix is symmetric, and as we are not interested in matching features with themselves or their mirrored equivalents, we only need to calculate the upper off-diagonal portion of the matrix. We can also limit the necessary comparisons by only attempting to match features whose scales are sufficiently similar for them to exhibit significant symmetry.

The number of matches per feature is not limited by the algorithm. Using only one match per feature works well in most situations. However, when there are repeated objects in the scene, or when searching for rotational symmetry of order greater than two there are obvious reasons to allow more than one match per feature. There is little additional computational load to generate several matching pairs per feature — the comparisons have been computed already — the only extra work is determining the symmetry for the additional pairs, which is extremely fast.

Allowing more than one match per feature allows the feature matching some degree of leeway when finding the correct match, however, it also increases the chance that incorrect "fluke" matches will be found that align with a dominant symmetry foci and are incorrectly grouped into a symmetric constellation. For our experiments we allowed one match per feature when detecting bilateral symmetry and four matches per feature when detecting rotational symmetry.

4   Performance

The new method was implemented in Matlab, with feature points detected and described using Lowe's SIFT code [16], and applied to detect bilateral and rotational symmetries in a diverse range of real images. Bilateral symmetry detection results are shown in Figure 6 and rotational symmetry detection results are shown in Figure 7.
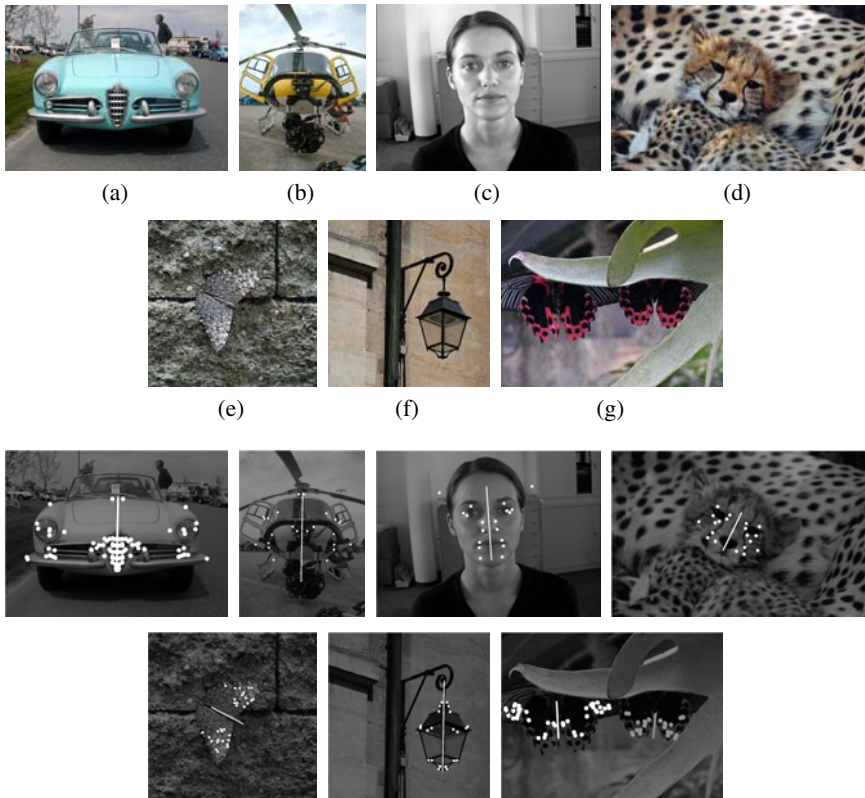
Fig. 6. Bilateral symmetry detection

Many objects and creatures exhibit a high degree of bilateral symmetry, especially
when viewed from the front or rear, this is particularly common for moving objects (and
creatures) whose dynamics benefit from symmetry about their direction of motion. In
Figure 6 we see examples of this with the detection of vehicles (a) and (b), and faces of
a person (c) and a cheetah (d). The symmetry axes detected together with the pairs of
reflective feature points contributing to the symmetry axis are illustrated. Figure 6 (d)
and (e) show creatures being detected with significant background clutter, (e) is partic-
ularly interesting as the subject appears partially camouflaged to a human eye. Many
static artefacts also exhibit symmetry such as the street lamp in Figure 6 (f). Figure 6 (g)
demonstrates the method detecting multiple axes of symmetry. When multiple axes are
drawn the brightness indicates the relative symmetry magnitudes of the constellations.

Figure 7 shows five images containing rotationally symmetric objects. The second
row shows the centres of rotational symmetry detected in each image, the feature points
associated with each centre of rotation, and arcs indicating the rotations linking match-
ing feature pairs. Figures 7 (a) and (b) illustrate the algorithm's ability to detect rota-
tionally symmetric objects in cluttered scenes, (c) and (d) show the method applied to
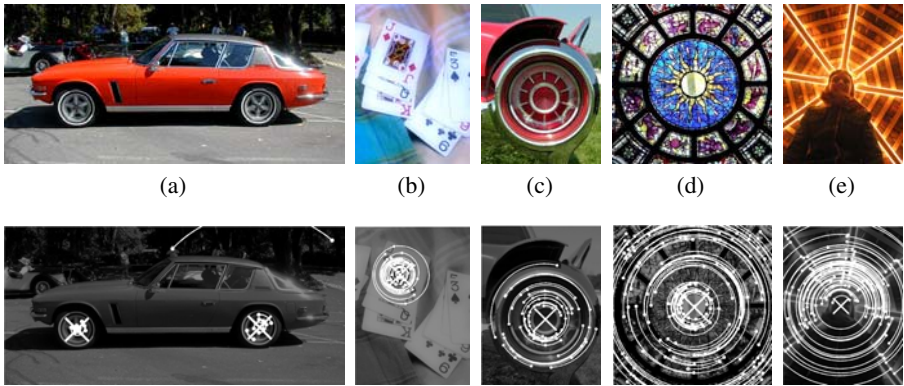
Fig. 7. Rotational symmetry detection. Estimated orders of rotational symmetry for detected centres: (a) 5 and 5, (b) 2, (c) 10, (d) 4, and (e) 8.
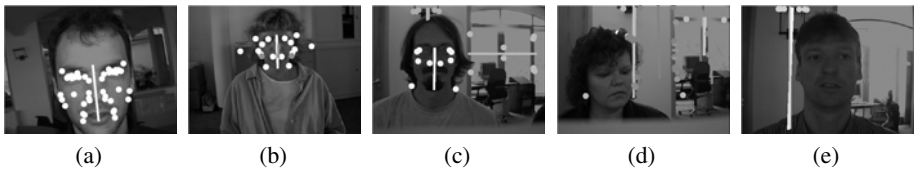

Fig. 8. Some results from the BioID database where the bilateral symmetry of the face was detected in 95.1% of cases, e.g. (a)-(c), and not detected in 4.9%, e.g. (d) and (e)

images with global and almost-global rotational symmetry, and (e) shows the method detecting rotational symmetry under partial occlusion. The orders of symmetry detected are also shown. Note that the order detected for (d) is 4 not 12, this is due to the cropping of the symmetric figure by the square image border which has left numerous features in the corners of the image with order 4 rotation.

To give an indication of the method's robustness it was applied to detect axes of symmetry in 1521 images from the BioID face database[2]. Ground truth symmetry axes were determined from 20 facial feature points manually annotated on each image[3]. Up to five symmetry axes were detected per image, and the axis of facial symmetry was deemed detected if the (r, θ) values of at least one detected axis lay within ± 5 pixels and $\pm 5^o$ of the ground truth respectively. Figure 8 shows some results. The symmetry axes of the faces were correctly identified in 95.1% of the images. The 4.9% of cases where the symmetry of the faces were not detected (e.g. Figure 8 (d) and (e)) were attributed to the non-symmetric appearance of facial features in some of the images, or insufficient feature points on the face due to lack of contrast. Note that other (non-facial) axes of symmetry detected in the images still exhibited a degree of symmetry.

---

[2] http://www.bioid.com/downloads/facedb

[3] FGNet Annotation of the BioID Dataset http://www-prima.inrialpes.fr/FGnet/

The performance of the new algorithm is closely linked to the matching capability of the feature method used, and it is important to generate a substantial number of feature points on a symmetric object for it to be reliably detected. In essence our method is matching instances of locally symmetric texture, so it works very well when applied to detailed two-dimensional symmetric patterns such as butterfly wings (Figure 3 and Figure 6 (e) and (g)), however, it works equally well for three-dimensional features when these features form symmetric patterns in an image, such as the face, lamp and vehicles in Figure 6. The method works less well for smooth textureless objects where the number of feature points diminishes. It is feasible, however, that a shape-based descriptor, such as [7], could provide sufficient features in such circumstances.

The new method is simple and fast with the majority of time consumed in computing features and performing the matching. The computational order for matching n feature points is $O(n^2)$, although the number of computations is reduced by only matching across similar scales. If a non-unity distance weighting D_{ij} (Equation 3) is used the squared distance between pairs can be used to further limit the number of comparisons necessary. This would be useful when searching for relatively small symmetric objects in large scenes. The image can then be divided into grid squares as wide as the maximum expected symmetry diameter and features need only be matched against features in the same or adjacent grid regions. However, at present with no such constraints, and running unoptimised Matlab code on a 2.8 GHz Pentium 4, the method is quite fast, e.g. it takes less than 1.5 seconds to compute symmetry in the image in Figure 6 (c) with 314 feature points, and under 7 seconds to compute the symmetry in Figure 3 with 946 feature points. The majority of time is spent generating and matching the features, for Figure 3 this takes 1 and 5.5 seconds respectively (SIFT feature generation is done by calling Lowe's pre-compiled C code [16]).

There is a great deal of opportunity to extend the approach presented here. The symmetric constellations of features, together with the accurate characterisation of symmetry foci, provide a strong basis for segmenting the symmetric regions. One possibility is to generate additional feature points in the vicinity of the symmetric matches, verify their symmetry and grow symmetric regions, in a similar fashion to Ferrari *et al.*'s object segmentation approach [4]. Segmenting the symmetric regions would also provide a more accurate measure of the extent of the axes of symmetry in the image.

5   Conclusions

A method has been presented that finds symmetric constellations of features in images and allows efficient computation of symmetries in the image plane. Its performance has been demonstrated on a diverse range of real images. The method simultaneously considers symmetries over all locations, scales and orientations, and was shown to reliably detect both bilaterally and rotationally symmetric figures in complex backgrounds, and handle multiple occurrences of symmetry in a single image. The method relies on the robust matching of feature points generated by modern feature techniques such as SIFT [16]. However, it is not restricted to any one such technique, rather, it provides a means to compute symmetry from features, with the requirements that these features facilitate orientation invariant matching and have an associated orientation measure.

The pair-wise matching underpinning this approach accounts for its efficiency, allowing symmetric pairs to "vote" for symmetry foci rather than having to search the space of all possible symmetries. Symmetric features are grouped into constellations based on their underlying symmetry, characterising both the symmetries present and identifying the features associated with each incidence of symmetry.

References

1. Stefan Carlsson. Symmetry in perspective. In *ECCV (1)*, pages 249–263, 1998.
2. Steven C. Dakin and Andrew M. Herbert. The spatial region of integration for visual symmetry detection. *Proc of the Royal Society London B. Bio Sci*, 265:659–664, 1998.
3. Larry S. Davis. Understanding shape, ii: Symmetry. *SMC*, 7:204–212, 1977.
4. V. Ferrari, T. Tuytelaars, and L. Van Gool. Simultaneous object recognition and segmentation from single or multiple model views. *Int. J. of Comp. Vis.*, 2005.
5. R. I. Hartley and A. Zisserman. *Multiple View Geometry in Computer Vision*. Cambridge University Press, ISBN: 0521540518, second edition, 2004.
6. W. Hong, A. Y. Yang, K. Huang, and Y. Ma. On symmetry and multiple-view geometry: Structure, pose, and calibration from a single image. *Int. J. of Comp. Vis.*, 2004.
7. F. Jurie and C. Schmid. Scale-invariant shape features for recognition of object categories. In *CVPR*, 2004.
8. L. Kaufman and W. Richards. Spontaneous fixation tendencies of visual forms. *Perception and Psychophysics*, 5(2):85–88, 1969.
9. Yan Ke and Rahul Sukthankar. Pca-sift: A more distinctive representation for local image descriptors. In *CVPR (2)*, pages 506–513, 2004.
10. Yosi Keller and Yoel Shkolnisky. An algebraic approach to symmetry detection. In *ICPR (3)*, pages 186–189, 2004.
11. N. Kiryati and Y. Gofman. Detecting symmetry in grey level images: The global optimization approach. *Int. J. of Comp. Vis.*, 29(1):29–45, August 1998.
12. Andreas Kuehnle. Symmetry-based recognition of vehicle rears. *Pattern Recognition Letters*, 12(4):249–258, 1991.
13. S. Lazebnik, C. Schmid, and J. Ponce. Semi-local affine parts for object recognition. In *BMVC*, 2004.
14. J. Liu, J. Mundy, and A. Zisserman. Grouping and structure recovery for images of objects with finite rotational symmetry. In *ACCV*, volume I, pages 379–382, 1995.
15. P. Locher and C Nodine. Symmetry catches the eye. In J. O'Regan and A Lévy-Schoen, editors, *Eye Movements: from physiology to cognition*. Elsevier, 1987.
16. David G. Lowe. Distinctive image features from scale-invariant keypoints. *Int. J. of Comp. Vis.*, 60(2):91–110, 2004.
17. Gareth Loy and Alexander Zelinsky. Fast radial symmetry for detecting points of interest. *IEEE Trans Pat. Rec. & Mach. Int.*, 25(8):959–973, August 2003.
18. M. Mancas, B. Gosselin, and B. Macq. Fast and automatic tumoral area localisation using symmetry. In *Proc. of the IEEE ICASSP Conference*, 2005.
19. G. Marola. On the detection of the axes of symmetry of symmetric and almost symmetric planar images. *IEEE Trans Pat. Rec. & Mach. Int.*, 11(1):104–108, January 1989.
20. T. Masuda, K. Yamamoto, and H. Yamada. Detection of partial symmetry using correlation with rotated-reflected images. *Pattern Recognition*, 26(8):1245–1253, August 1993.
21. K. Mikolajczyk and C. Schmid. A performance evaluation of local descriptors. *IEEE Trans Pat. Rec. & Mach. Int.*, pages 1615–1630, October 2005.

22. K. Mikolajczyk, T. Tuytelaars, C. Schmid, A. Zisserman, J. Matas, F. Schaffalitzky, T. Kadir, and L. Van Gool. A comparison of affine region detectors. *Int. J. of Comp. Vis.*, 2006.
23. S. Mitra and Y. Liu. Local facial asymmetry for expression classification. In *CVPR*, 2004.
24. D. Reisfeld, H. Wolfson, and Y. Yeshurun. Context free attentional operators: the generalized symmetry transform. *Int. J. of Comp. Vis.*, 14(2):119–130, 1995.
25. R. Scognamillo, G. Rhodes, C. Morrone, and D. Burr. A feature-based model of symmetry detection. *Proc R Soc Lond B Biol Sci*, 270:1727–33, 2003.
26. G. Scott and H. C. Longuet-Higgins. Feature grouping by "relocalisation" of eigenvectors of the proximity matrix. In *BMVC*, pages 103–108, 1990.
27. Gal Sela and Martin D. Levine. Real-time attention for robotic vision. *Real-Time Imaging*, 3:173–194, 1997.
28. D. Sharvit, J. Chan, H. Tek, and B. B. Kimia. Symmetry-based indexing of image databases. In *Proc. IEEE Workshop on Content-Based Access of Image and Video Libraries*, 1998.
29. D. Shen, H.H.S. Ip, and E.K. Teoh. Robust detection of skewed symmetries. In *ICPR*, volume 3, pages 1010–1013, 2000.
30. D.G. Shen, H.H.S. Ip, and E.K. Teoh. Affine invariant detection of perceptually parallel 3d planar curves. *Pattern Recognition*, 33(11):1909–1918, November 2000.
31. C. Sun and D. Si. Fast reflectional symmetry detection using orientation histograms. *Journal of Real Time Imaging*, 5(1):63–74, February 1999.
32. Tinne Tuytelaars, Andreas Turina, and Luc J. Van Gool. Noncombinatorial detection of regular repetitions under perspective skew. *IEEE Trans Pat. Rec. & Mach. Int.*, 25(4):418–432, 2003.
33. C. W. Tyler, L. Hardage, and R. T. Miller. Multiple mechanisms for the detection of mirror symmetry. *Spatial Vision*, 9(1):79–100, 1995.
34. A.Y. Yang, S. Rao, K. Huang, W. Hong, and Y. Ma. Geometric segmentation of perspective images based on symmetry groups. In *ICCV*, pages 1251–1258, 2003.
35. R.K.K. Yip. A hough transform technique for the detection of reflectional symmetry and skew-symmetry. *Pattern Recognition Letters*, 21(2):117–130, February 2000.
36. H. Zabrodsky, S. Peleg, and D. Avnir. Completion of occluded shapes using symmetry. In *CVPR*, pages 678–679, 1993.
37. Hagit Zabrodsky, Schmuel Peleg, and David Avnir. Symmetry as a continuous feature. *IEEE Trans Pat. Rec. & Mach. Int.*, 17(12):1154–1166, December 1995.
38. T. Zielke, M. Brauckmann, and W. von Seelen. Intensity and edge-based symmetry detection with an application to car-following. *CVGIP: Image Underst.*, 58(2):177–190, 1993.